Multilevel Power Electronic Systems Adjusted by Algorithms of Multi-Zone Space-Vector Modulation: A Survey

Valentin Oleschuk, Mihai Tirsu, Irina Vasiliev
Institute of Power Engineering of Moldova
Chisinau, Republic of Moldova

Abstract **-This publication provides a brief overview of the results of dissemination of the method of multi-zone space-vector pulse-width modulation (PWM) for the adjustment of inverter-based installations (with low switching frequency of inverters) characterized by multilevel output voltage: a) of split-phase variable speed drives; b) of transport-oriented ac drives with two windings of the stator of electrical machine; c) of three-inverter-based power systems with modular configuration; d) of photovoltaic (PV) systems with twin inverters; e) of five-phase installations with asynchronous machine with open-end winding; f) of six-phase structures with quad inverters, and g) of photovoltaic installations based on triple inverters and transformer of multi-winding configuration. It has been shown that the developed schemes, techniques, and algorithms of multi-zone synchronous PWM (MZS PWM) applied for control of the mentioned above inverter-based systems (with specialized phase-shift between signals of separate inverters) assure synchronization and symmetry of the basic voltage waveforms of installations over the entire control range. It provides minimization of unwanted sub-harmonics (of the operating frequency) in spectral composition of the basic voltages of these installations, leading to reducing of losses in systems and to increasing of its efficiency.**

Keywords—pulse width modulation inverters, variable speed drives, photovoltaic systems, voltage control, spectral analysis.

I. Introduction

Power electronic converters are the main operating mechanisms of multiple industrial, traction, and residential installations. Therefore, wide applications in transport-focused variable speed drives have now dual three-phase installations with two voltage source inverters (VSI) [1] – [3]. Also, ones of perspective topology of drives are two-inverter-based apparatuses with electric machine with open-end winding, which are characterized by reduced common mode voltage/zero sequence voltage in these installations [4] – [6].

Actively developed in recent years are five-phase equipment based on five-phase inverters, which are characterized by increased reliability of operation [7] – [9]. Also, one of the promising varieties of controlled electric drives are installations based on two VSIs with two stator windings of asynchronous electric motor [10], [11].

The areas of the most expedient use of six-phase installations with four (quad) VSIs are powerful ac electric drives for traction application [12] – [14]. It should be noted that in this area, also converters of a modular type based on three VSIs and intermediate transformer can be used [15], [16].

With regard to photovoltaic systems, promising structures for high-power systems include two-inverter-based installations with multilevel voltage, including structures with double-delta configuration of inverter-side windings of the transformer [17], [18]. Also, three-inverter-based photovoltaic systems can be used in the corresponding transformer-based power conversion apparatuses [19], [20].

All topologies of the above-mentioned power electronic converters are based on the use of powerful semiconductor switches (transistors and thyristors) operating in a pulsed mode. In accordance with this, the parameters and characteristics of converters and the corresponding systems depend on the methods, schemes, and techniques of pulse-width modulation applied for generation of control signals (pulse control signals) of the converters used in the systems.

In order to improve the harmonic (spectral) composition of the output voltage of inverter-based systems, a new method of MZS PWM has been developed, which assures providing minimization of even-order harmonics and unwanted sub-harmonics (of the operating frequency) in voltage spectra of converters [21], [22].

In this publication, a brief review of the results of recent research in the field of development and dissemination of the method of MZS PWM, based on space-vector approach, in relation to the converters of the above-mentioned ac drive systems and photovoltaic installations, published in [23] – [42], is carried out. It is necessary to mention, that the using of algorithms of MZS PWM is the most perspective in installations with low switching frequency (SF) of VSIs.

II. Method of Synchronous Multi-Zone Modulation

An alternative method of MZS PWM (based mainly on space-vector approach) of pulse signals of VSIs makes it possible to assure synchronous character of processes of modulation in systems, insuring symmetry of the output voltage of VSIs over the entire control diapason [23].

Table I presents the basic parameters and functional relationships for determining the values of the control signals of inverters with MZS PWM in relation to the scalar operating mode of three-phase, six-phase, and five-phase regulated drive systems [23]. Fig. 1 shows (within a 60-degree clock interval) the state diagram of the keys of a three-phase inverter (switching state sequence (SStS)), as well as the curves of the line voltage (V_{ab}), and pole voltages (V_a, V_b) of VSI adjusted by algorithms of continuous MZS PWM [23].

TABLE I. CONTROL FUNCTIONS AND PARAMETERS OF CONTROL SIGNALS OF DRIVE VSIS ADJUSTED BY ALGORITHMS OF MZS PWM [23]

Control function	Three--phase and six-phase inverters	Five-phase inverters
Basic parameters	F – fundamental frequency of system F_m – maximum operating frequency of system τ - sub-switching interval	
Modulation index for scalar control	$m = F / F_m$	
Boundary frequencies transient between PWM sub-zones	$F_i = \frac{1}{6(2i-1)\tau}$ $F_{i-1} = \frac{1}{6(2i-3)\tau}$	$F_i = \frac{1}{10(2i-1)\tau}$ $F_{i-1} = \frac{1}{10(2i-3)\tau}$
Index of synchronization	$K_s = 1 - \frac{F - F_i}{F_{i-1} - F_i}$	
The central switch-on state	$\beta_1 = 1.10 m\tau$	$\beta_1 = 1.21 m\tau$
Others switch-on states	$\beta_j = \beta_1 \times \cos[(j-1)\tau]$	$\beta_j = \gamma_j^{'} + \gamma_j^{''} + \delta_j^{'} + \delta_j^{''} = 1.618\beta_1 \cos[(j-1)\tau]$
Border's active switching state	$\beta'' = \beta_1 \times \cos[(k-1)\tau]K_s$	$\beta'' = 1.618\beta_1 \times \cos[(k-1)\tau]K_s$
The minor part of switch-on states	$\gamma_k = \beta_{i-k+1}[0.5 - 0.9\tan(i-k)\tau]$	$\delta_k{'} + \delta_k{''} = 0.382\beta_{i-k+1}$
Switch-off (zero) states	$\lambda_j = \tau - (\beta_j + \beta_{j+1})/2$	
Boarder's switch-off state	$\lambda_i = \lambda^{'} = (\tau - \beta^{''})K_s$	

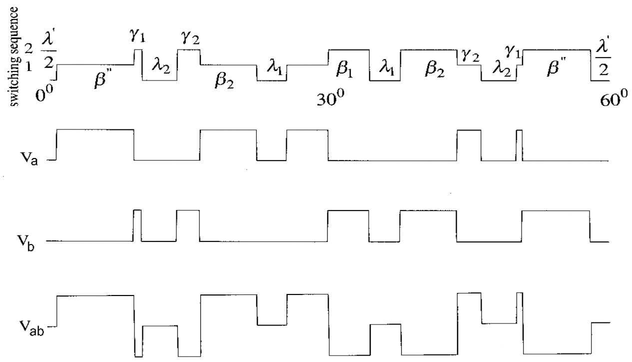

Fig. 1. SStS and basic voltages (inside a 60-degree diapason) of three-phase VSI with continuous MZS PWM [23].

The process of determining the parameters of inverter control signals (pulse signals) for three-phase/six-phase systems with MZS PWM is based on the continuous calculation of the values $F_i = \frac{1}{6(2i-1)\tau}$ и $F_{i-1} = \frac{1}{6(2i-3)\tau}$ of intermediate frequencies between the sub-ranges (sub-zones) of regulation (as a function of the duration of the clock subinterval τ), and in the calculation of the synchronization coefficient $K_s = [1 - (F - F_i)/(F_{i-1} - F_i)]$, which is an important component of the basic functional relationships (Table I) [23].

III. SPLIT-PHASE DRIVE SYSTEM WITH INVERTERS CONTROLLED BY MZS PWM [23], [29], [36], [40]

Fig. 2 shows topology of traction drive base on split-phase induction machine feeding by two three-phase VSIs supplied by insolated dc sources with unequal dc voltages ($V_{dc1} = 0.5V_{dc2}$) [29]. Figs. 3–4 show basic waveforms of voltages and of the phase current, and also its spectra, for the system with the *10kW* asymmetrical split-phase electric machine, regulated by algorithms of continuous MZS PWM. Operating frequency of installation is equal to *40Hz*, and SF of VSIs is equal to *1050Hz* [29].

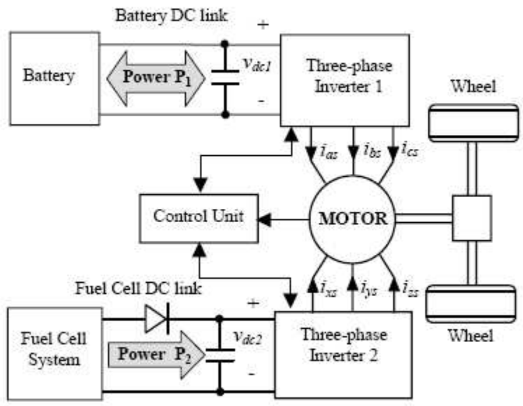

Fig. 2. Two VSI-based split-phase traction system [29].

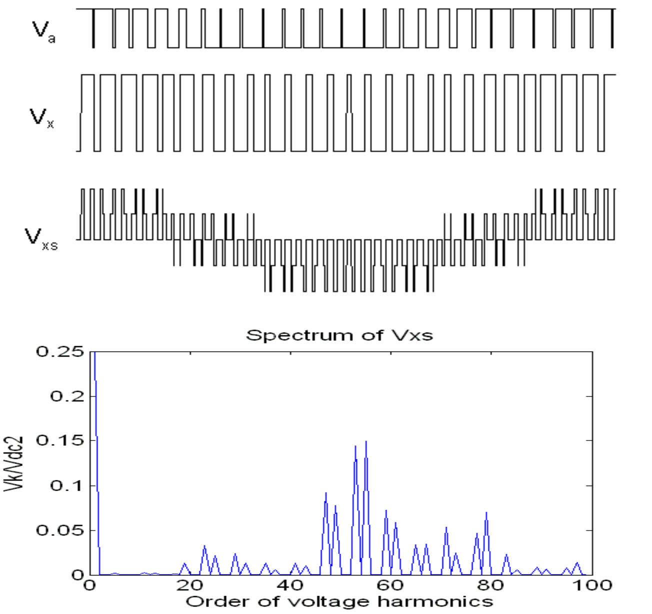

Fig. 3. Pole voltages of VSIs (V_a, V_x), and phase voltage of system V_{xs} (with its spectrum) for traction drive with continuous MZS PWM [29].

The presented diagrams and spectrograms prove the fact, that waveforms of the basic voltages of the analyzed drive installation have symmetry (quarter-wave symmetry in this case) over the entire adjustment range, and its spectrum, and also spectrum of the phase current, does not contain even-order voltage and current harmonics and unwanted sub-harmonics. So, these factors have particular importance in the case of elaboration of power traction systems with low SF of VSIs.

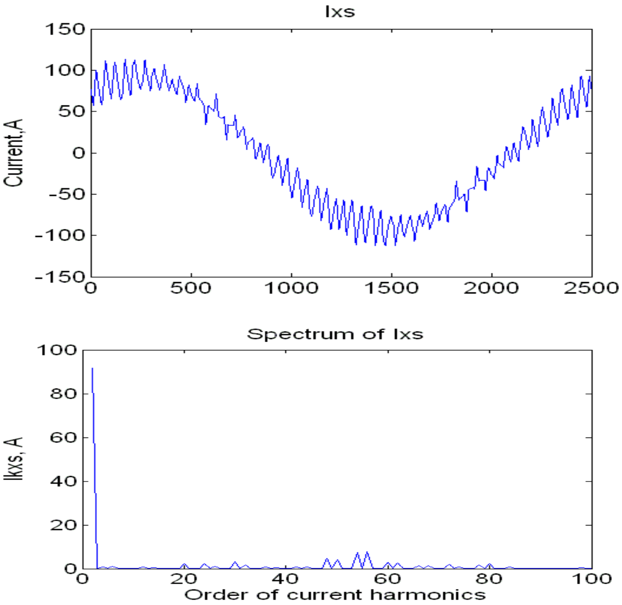

Fig. 4. Phase current I_{xs} of split-phase system, together with its spectrum, for traction drive controlled by continuous MZS PWM [29].

IV. VSI-Based Drive with Electrical Machine with Two Stator Windings [33] – [35], [37], [42]

One of the promising structures for ac drives of increased power is system based on two inverters, the output circuits of which are connected respectively to two stator windings of an asynchronous electric motor, characterized by a specialized connection of the stator windings of the motor to each other according to the double triangle scheme (Fig. 5) [34].

Figs. 6-7 present the results of modeling of processes in a system based on two inverters with synchronous continuous space-vector modulation (PWMC), feeding two stator windings of the induction machine [34]. In particular, Fig. 6 shows the diagrams of the base voltages in this installation, and Fig. 7 presents the spectrogram of the resulting voltage V_{w11} on the stator winding of the induction machine. The operating frequency of the system is equal to $F = 32.5Hz$, the modulation index of VSIs is equal to $m = 0.65$, and average SF of VSIs is equal to $F_s = 1050Hz$.

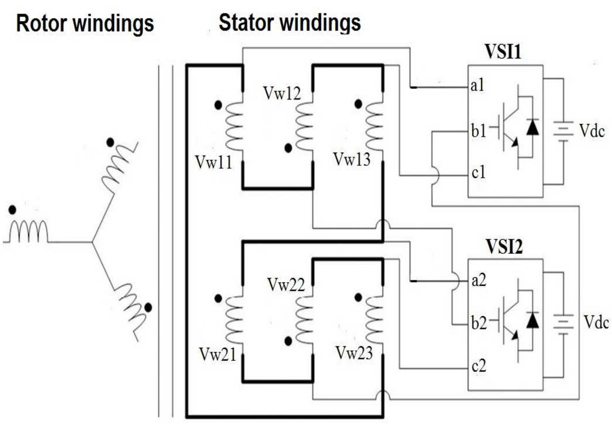

Fig. 5. Topology of drive installation with two VSIs [34].

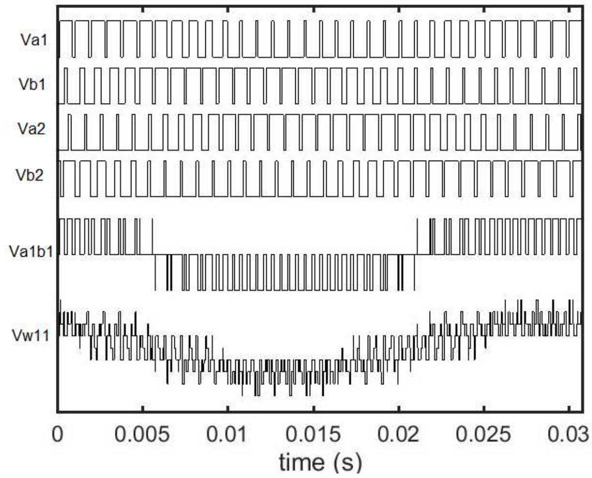

Fig. 6. Basic voltages of system with continuous MZS PWM [34].

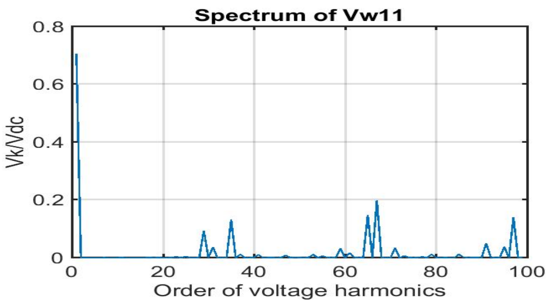

Fig.7. Spectrum of the winding voltage [34].

It should be noted that the analyzed mode of operation of a two-inverter system is characterized by a fractional ratio between the switching frequency of the inverters F_s and the system output frequency F ($F_s/F = 1050Hz/32.5Hz = 32.31$). The results presented in Fig. 7 confirm the fact that even for operating modes with a fractional relationship between SF of VSIs and the output frequency of the system, the upgraded techniques of MZS PWM make it possible to provide an improved harmonic composition of the voltage on the stator windings of the motor, spectrum of which do not contain even-order voltage harmonics, as well as unwanted sub-harmonics (of the operating frequency).

Fig. 8 presents the results of calculation of Weighted Total Distortion Factor (*WTHD*) of the base voltages V_{a1b1} and V_{w11} in two-VSI-based installation adjusted by the scheme of MZS PWM ($WTHD = (1/V_{w11_1})\sqrt{\sum_{i=2}^{1000}(V_{w11i}/i)^2}$), operating under scalar control mode, as a function of the modulation index m of inverters, SF of VSIs is equal to *1050Hz* in this case [34]. Thus, it is shown that at low and medium values of modulation index of VSIs ($m < 0.65$), algorithms of continuous MZS PWM (PWMC) allow insuring the best integral spectral characteristics of the winding voltage V_{w11}. At higher values of index of modulation ($m > 0.65$), an improved integral characteristics of spectrum of winding voltage of the motor is achieved using modified techniques of discontinuous MZS PWM (PWMD) [34].

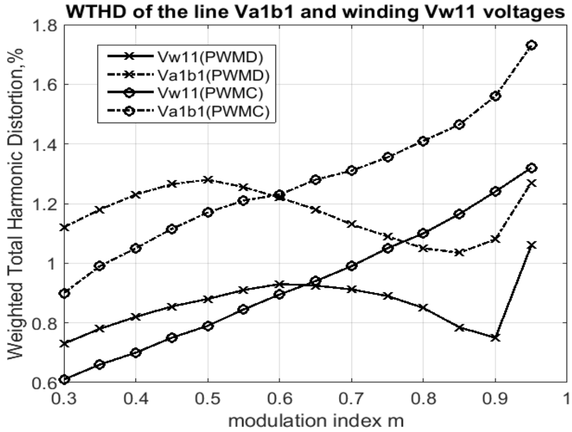

Fig. 8. *WTHD* of voltages of two-VSI-based installation [34].

V. Five-Phase Drive Installation with Two VSIs Adjusted by MZS PWM [26], [29], [36], [42]

Fig. 9 shows the structure of a five-phase electric drive, which includes two five-phase VSIs with two separate power supplies, and outputs of VSIs are connected to the corresponding terminals of the open windings of a five-phase asynchronous electric motor [26]. Fig. 9 shows also basic space-vector diagram of a five-phase VSI, which is the basis for the synthesis of rational control and modulation schemes, including schemes and techniques of MZS PWM, in five-phase structures [26].

Fig. 10 presents the basic voltages of a five-phase system with operating frequency equal to *39.7Hz* and SF of VSIs equal to *2300Hz*, controlled by algorithms of MZS PWM [26]. Fig. 11 presents spectrogram of the phase voltage of five-phase drive installation, which contains only odd-order voltage harmonics [26].

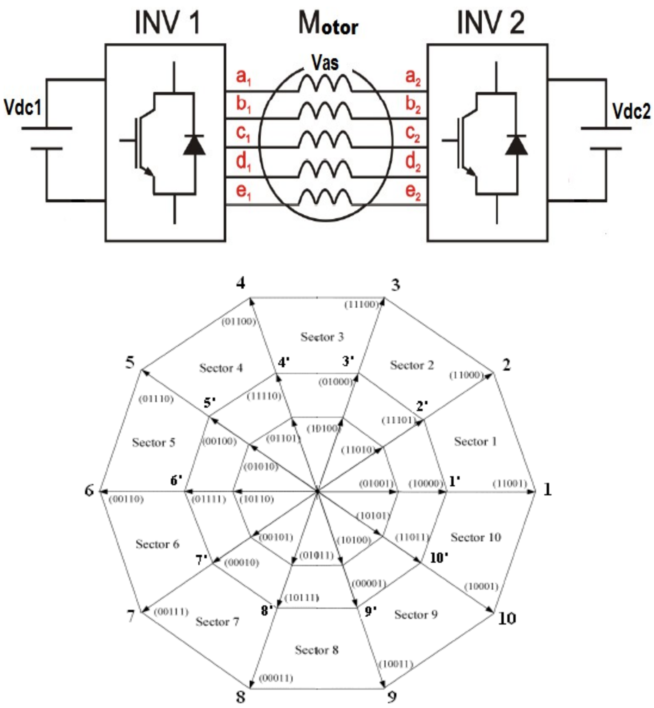

Fig. 9. Topology of five-phase open-end winding drive installation, and its space-vector diagram [26].

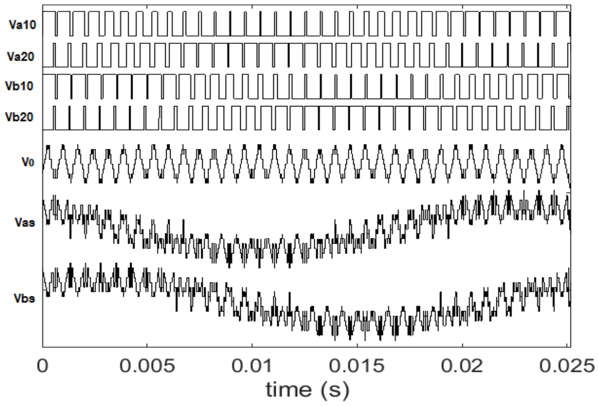

Fig. 10. Base voltages in five-phase installation adjusted by algorithms of MZS PWM [26].

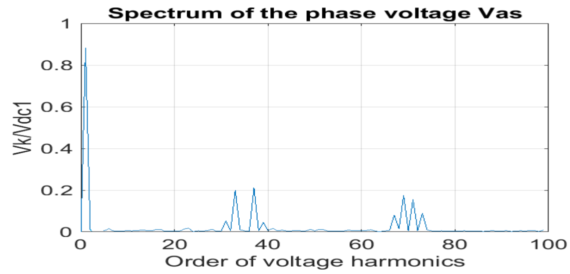

Рис. 11. Voltage spectrum of five-phase installation [26].

Thus, the use of algorithms of MZS PWM makes it possible to eliminate unwanted subharmonics from spectrum of the phase voltage of open-end winding five-phase drive apparatuses.

VI. Six-Phase Installation Based on Four VSIs Adjusted by the Scheme of MZS PWM [25], [27], [31], [40]

One of the promising topologies of converter systems for the medium-power variable speed drive with increased power rating is shown in Fig. 12 six-phase installation with open windings of an asymmetric asynchronous electric machine, containing two sets of three-phase windings spatially shifted by 30 electrical degrees relative to one another [40]. Also, four VSIs (INV1 - INV4 in Fig. 12), and four insulated dc sources, are basic parts of this drive configuration [40].

Fig. 13 and Fig. 14 show the results of modeling of processes in a six-phase system based on four power supplies with voltages V_{dc1} - V_{dc4}, and four two-level VSIs adjusted by algorithms of MZS PWM for a specific control mode of inverters, characterized by the adjustment of the SF of the switches of each VSI F_{s1} - F_{s4} through its functional interconnection with value of voltages of the corresponding dc source. Fig. 13 presents the normalized values of the basic voltages of installation. Fig. 14 shows spectrograms of multilevel phase and line voltages of six-phase drive [40].

Thus, the use of techniques of MZS PWM algorithms for controlling VSIs of six-phase installations makes it possible to ensure symmetry of waveforms of the phase voltage of apparatuses over the entire control diapason and under any operating conditions of installation. In the phase voltage spectrum there are lacking in this case even voltage harmonics and unwanted sub-harmonics, which is especially important for systems based on VSIs with low SF.

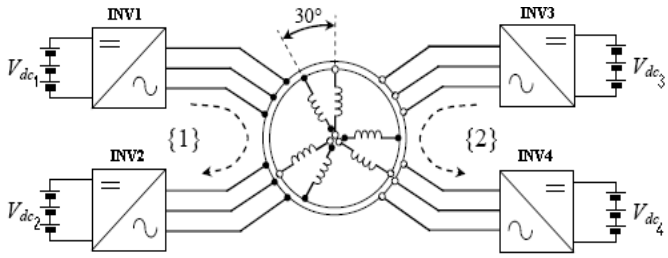

Fig. 12. Topology of six-phase installation on the base of four VSIs [40].

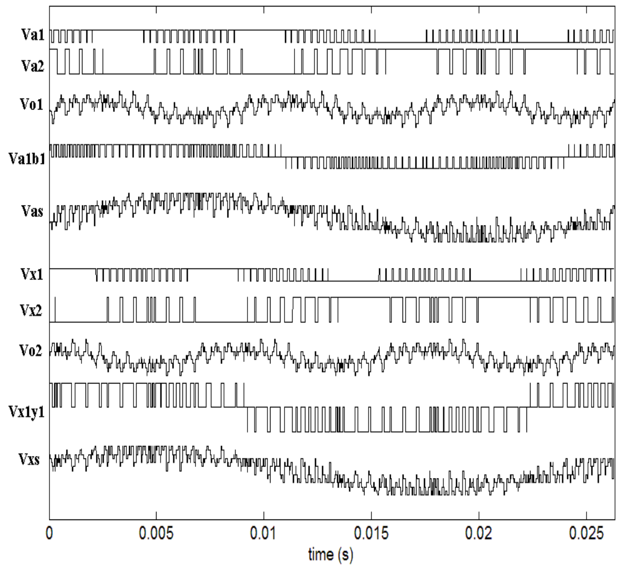

Fig. 13. Basic voltages of six-phase apparatus adjusted by MZS PWM (F = $38Hz$, $F_{s2} = F_{s4} = 1000Hz$, $F_{s1} = F_{s3} = 2000Hz$, $V_{dc2} = V_{dc4}$, $V_{dc1} = 0.50V_{dc4}$, $V_{dc3} = 0.50V_{dc4}$) [40].

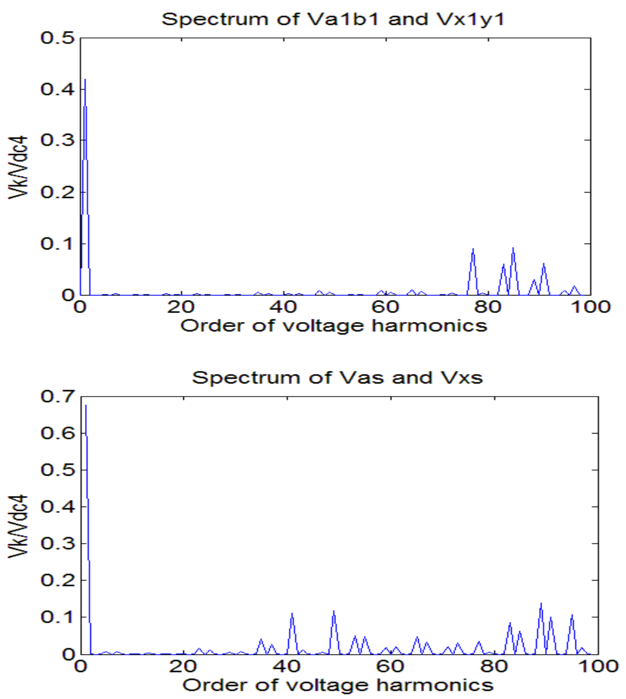

Fig. 14. Spectra of the line-to-line (V_{a1b1}, V_{x1y1}) and phase (V_{as}, V_{xs}) voltages of six-phase installation with algorithms of MZS PWM [40].

VII. Modular Converters with Three VSIs Adjusted by the Scheme of MZS PWM [24], [28], [42]

One of configurations of modular converters consists from three VSIs, outputs of which are specially connected with the corresponding windings of a 0.33 p.u. intermediate transformer [15], [16].

Results of investigation of operation of a modular converter based on three two-level VSIs adjusted by techniques of modified MZS PWM show, that the developed schemes of multi-zone modulation assure providing an improved spectral composition of the multi-level voltage at the load of modular installations [24], [42].

Also, in [28], a study of operation of modular installation with triple neutral-point-clamped converters adjusted by specialized algorithms of MZS PWM, has been executed.

VIII. Two-Inverter-Based Photovoltaic Installation with Multi-Winding Power Transformer [30], [32], [38] – [39], [41]

Several configurations of power circuits of transformer-based photovoltaic (PV) systems based on two inverters are known [30, 41]. Fig. 15 shows the structure of PV installation with power transformer and with two VSIs, and in this case inverter-side windings of transformer have specific double delta configuration [32].

Fig. 16 shows the basic voltages in a PV system based on two VSIs adjusted by techniques of continuous MZS PWM (PWMC), as well as the spectral characteristics of the winding voltage V_{w11} of multi-winding transformer [32]. The output frequency of the system is equal to $50Hz$, and averaged SF of the inverters is $1050Hz$ [32].

Fig. 17 shows the results of determining the Total Harmonic Distortion factor (THD) of the line voltage and of the winding voltage of multi-winding transformer ($THD = (1/V_{w11_1})\sqrt{\sum_{k=2}^{100} V_{w11_k}^2}$) as a function of the modulation index m of VSIs, for three basic control modes of VSIs: for control mode with continuous MZS PWM (PWMC), and for two control regimes based on two discontinuous variants of MZS PWM (PWMD30 and PWMD60) [32]. Averaged SF of VSIs is equal to $1050Hz$ in these cases.

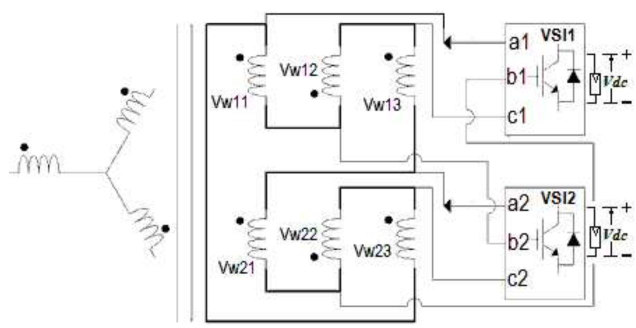

Fig. 15. Topology of PV apparatus with two VSIs [32].

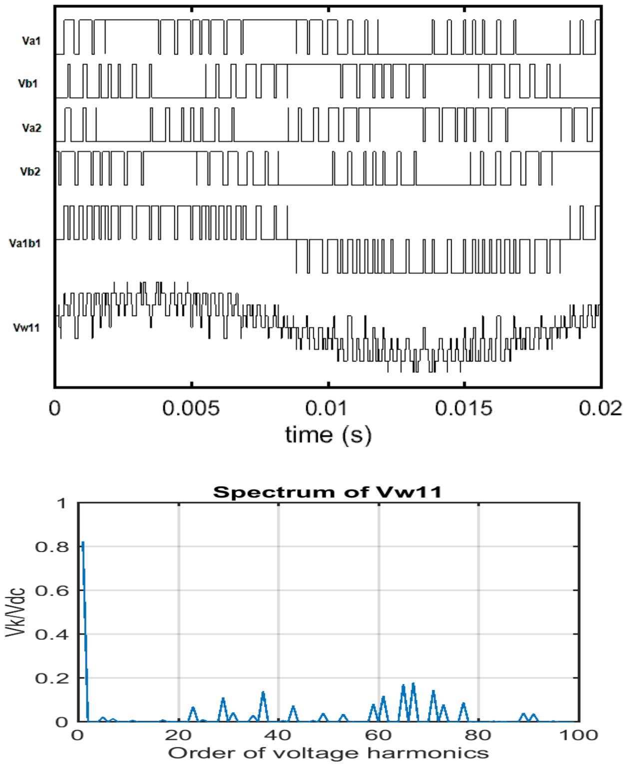

Fig. 16. Basic voltages of PV installation, and spectrum of the winding voltage V_{w11} [32].

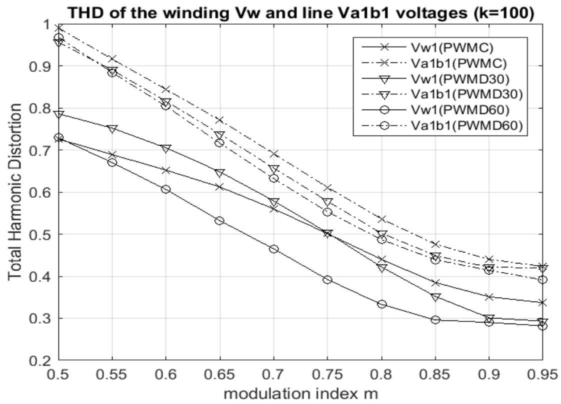

Fig. 17. *THD* of voltages versus coefficient of modulation of VSIs [32].

The presented results show that over most of the control diapason of a VSI-based PV installation, the best spectral characteristics of the voltage on the windings of multi-winding transformer are turns out for the cases of the using of techniques of discontinuous MZS PWM with the 60^0-non-switching notches (PWMD60 in Fig. 17) for adjustment of two VSIs [32].

IX. Three-Inverter-Based Photovoltaic Installations with Multi-Winding Power Transformer [30], [41]

Fig. 18 shows topology of PV installation based on a multi-winding transformer with a special connection of the corresponding windings of transformer to outputs of three VSIs supplied by the corresponding multi-string photovoltaic panels [30].

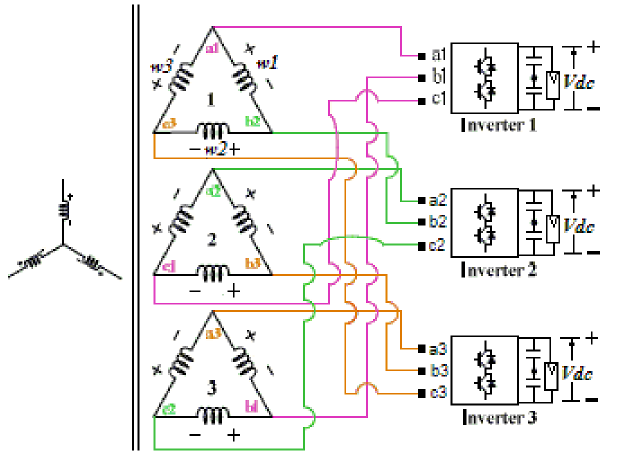

Fig. 18. Topology of PV apparatus with three modulated VSIs [30].

Figs. 19 - 20 show basic voltage waveforms (pole, phase, and line voltages, as well as the resulting winding voltage V_{w1line}) of PV installation with three VSIs controlled by algorithms of continuous MZS PWM (Fig. 19), and of discontinuous MZS PWM (Fig. 20) [30]. Fig. 19 and Fig. 20 present also spectrograms of the basic winding voltage V_{w1line} of PV installation with operating frequency equal to *50Hz*, and averaged SF of VSIs equal to *1130Hz*. Coefficient of modulation of VSIs is equal to *0.65* in this case [30].

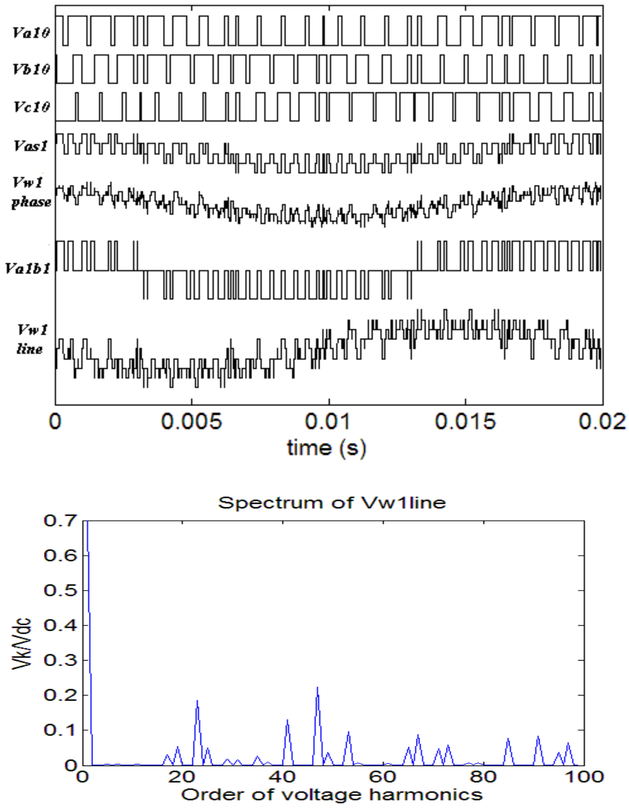

Fig. 19. Basic voltages and spectrum of the winding voltage of PV installation with three VSIs adjusted by the scheme of continuous MZS PWM (CPWM) [30].

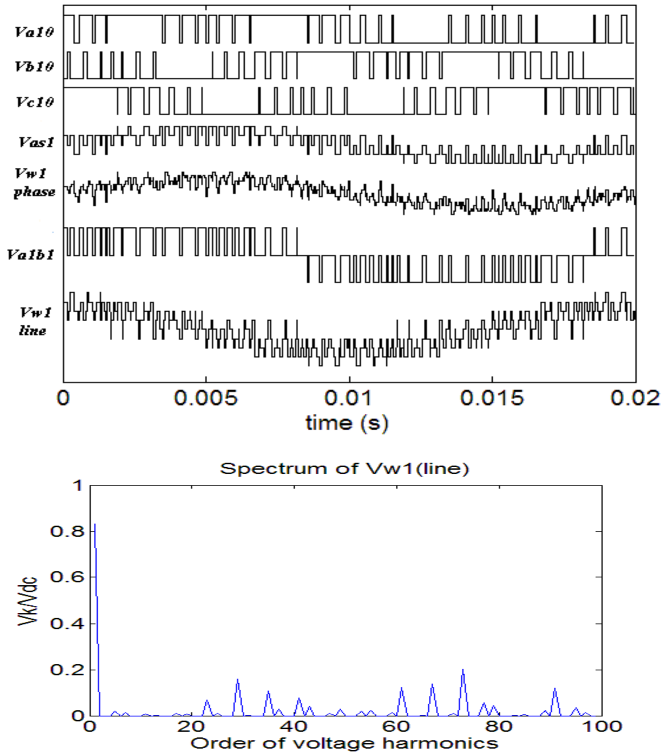

Fig. 20. Basic voltages and spectrum of the winding voltage of PV installation with three VSIs adjusted by the scheme of discontinuous MZS PWM (DPWM30) [30].

The presented in Figs. 19 - 20 spectrograms confirm the fact that there are no even harmonics and unwanted sub-harmonics (of the operating frequency) in spectra of the winding voltage of VSI-based PV system, which assure providing reduction of losses and increasing of efficiency of operation of this type of photovoltaic installations [30].

Fig. 21 presents the results of determining the Total Harmonic Distortion factor ($THD = (1/V_{w1_1})\sqrt{\sum_{k=2}^{40} V_{w1_k}^2}$) of basic voltages of PV system (of the line voltage V_{a1b1} and of the winding voltage V_{w1}) as a function of modulation index *m* of VSIs. Therefore, it presents results of determining of *THD* of voltages of PV system with three VSIs (SF = *1400Hz* in this case), adjusted both by technique of continuous MZS PWM (CPWM), and by two schemes of discontinuous MZS PWM (DPWM30 and DPWM60) [30].

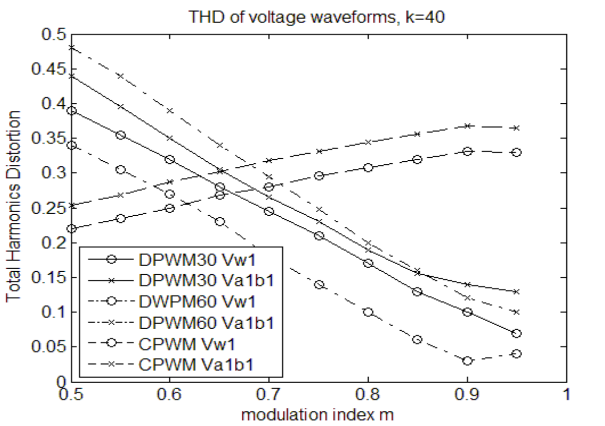

Fig. 21. *THD* of basic voltages of VSI-based PV installation [30].

Conclusion

New strategies, schemes, and algorithms of MZS PWM, developed, modified, and disseminated for adjustment of VSIs of three-phase, five-phase, and six-phase installations of variable speed drives of increased power (characterized by low SF of VSIs), as well as to the regulation of dual and triple inverters of transformer-based PV installations, allow insuring continuous synchronization and symmetry of the resulting multilevel voltages of the mentioned above systems over the entire control range.

In the spectra of the output voltage of VSIs, as well as in the spectra of the phase and line voltage of the corresponding power conversion systems with MZS PWM, there are no even-order harmonics and unwanted sub-harmonics. Improving the spectral composition of voltages and currents in these systems leads to redaction of losses in the corresponding installations and an increase in the efficiency of their operation. Therefore:

A. Algorithms of MZS PWM of signals of VSIs of power conversion installations of various functional purposes make it possible to insure synchronization and symmetry of the basic voltages of apparatuses at any ratio (integer or fractional) between SF of VSIs and the operating frequency of installations.

B. Schemes and algorithms of MZS PWM make it possible to assure the symmetry of the basic voltage waveforms in multi-inverter installations with unequal dc voltages of insulated autonomous dc sources.

C. Developed techniques of MZS PWM can be successfully applied for control of both systems based on standard two-level VSIs, of installations based on diode-clamped inverters, and of systems based on five-phase and six-phase VSIs.

D. Specialized schemes and algorithms of MZS PWM make it possible to ensure synchronization and symmetry of the basic voltages in VSI-based installations and apparatuses at increased, close to the maximum, values of the coefficient of modulation of VSIs operating in the overmodulation control zone.

References

[1] D. Hadiouche, L. Baghli, and A. Rezzoug, "Space-vector PWM techniques for dual three-phase AC machine: analysis performance evaluation and DSP implementation," IEEE Trans. Ind. Appl., vol. 42, no. 4, 2006, pp. 1112-1122.

[2] R. Bojoi, F. Farina, F. Profumo, and A. Tenconi, "Dual-three phase induction machine drives control – a survey," IEEJ Trans. on Industry Appl., vol. 126, no. 4, 2006, pp. 420-429.

[3] M. Jones, F. Patkar, and E. Levi, "Carrier-based pulse-width modulation techniques for asymmetrical six-phase open-end winding drives," IET Electric Power Appl., vol. 7, issue 6, 2013, pp. 441–452.

[4] M.R. Baiju, K.K. Mohapatra, R.S. Kanchan, and K. Gopakumar, "A dual two-level inverter scheme with common mode voltage elimination for an induction motor drive," IEEE Trans. on Power Electronics, vol. 19, no. 3, 2004, pp. 794-805.

[5] P. Sanjeevikumar, M.S. Bhaskar, P.K. Maroti, F. Blaabjerg, P. Siano, and V. Oleschuk, "Hexuple-inverter configuration for multilevel nine-phase symmetrical open-winding converter," Proc. of IEEE Int'l Conf. on Power Electronics, Intelligent Control, and Energy Systems (ICPEICES'2016), 2016, 6 p.

[6] R.P.R. de Sousa and C.B. Jacobina, "Open-end unidirectional topologies with reduced controlled switch count," Proc. of IEEE Applied Power Electronics Conf. and Exposition (APEC'2017), 2017, pp. 397-403.

[7] A. Iqbal and E. Levi, “Space vector modulation schemes for a five-phase voltage source inverter,” Proc. of European Conf. on Power Electronics and Application (EPE’2005), 2005, 12 p.

[8] J. Prieto, M. Jones, F. Barrero, E. Levi, and S. Toral, “Comparative analysis of discontinuous and continuous PWM techniques in VSI-fed five-phase induction motor,” IEEE Trans. Ind. Electron., vol. 58, no. 12, 2011, pp. 5324–5335.

[9] N. Bodo, E. Levi, and M. Jones, “Investigation of carrier-based PWM techniques for a five-phase open-end winding drive topology,” IEEE Trans. Ind. Electron., vol. 60, no. 5, 2013, pp. 2054-2065.

[10] Y. Park, J.-M. Yoo, and S.-K. Sul, “Double-delta sourced winding for dual winding induction machine,” Proc. of IEEE Int’l Conf. on Power Electronics - ECCE Asia (ICPE-ECCE Asia’2015), 2015, pp. 77-85.

[11] Y. Park, J.-M. Yoo, and S.-K. Sul, “Vector control of double-delta sourced winding for a dual-winding induction machine,” IEEE Trans. Ind. Appl., vol. 53, no. 1, 2017, pp. 171–180.

[12] G. Grandi, A. Tani, P. Sanjeevikumar, and D. Ostojic, “Multi-phase multi-level ac motor drive based on four three-phase two-level inverters,” Proc. of IEEE Int’l Symp. on Power Electronics, Electrical Drives, Automation and Motion (SPEEDAM’2010), 2010, pp. 1768–1775.

[13] A. Tani, G. Serra, M. Mengoni, L. Zarri, G. Rini, and D. Casadei, “Dynamic stator current sharing in quadruple three-phase induction motor drives,” Proc. of IEEE Industrial Electronics Society Conf. (IECON’2013), 2013, pp. 5173-5178.

[14] N.K. Kumar and K. Sivakumar, “A quad two-level inverter configuration for four-pole induction-motor drive with single DC link,” IEEE Trans. Ind. Electron., vol. 62, no. 1, 2015, pp. 105-112.

[15] M. Malinowski, K. Gopakumar, J. Rodriguez, and M.A. Pérez, “A survey on cascaded multilevel inverters,” IEEE Trans. Ind. Electron., vol. 57, no.7, 2010, pp. 2197-2206.

[16] Yin Li and Lingling Fan, “Modular multilevel converter based induction machine drive,” Proc. of IEEE North American Power Symp. (NAPS’2015), 2015, pp. 173-178.

[17] G. Grandi, C. Rossi, D. Ostojic, and D. Casadei, “A new multilevel conversion structure for grid-connected PV applications,” IEEE Trans. Ind. Electron., vol. 56, no. 11, 2009, pp. 4416–4426.

[18] Y. Park, S. Ohn, and S.-K. Sul, “Multi-level operation with two-level converters through a double-delta source connected transformer,” Journal of Power Electronics, vol. 14, no. 6, 2014, pp. 1093-1099.

[19] S. Ohn, Y. Park, and S.-K. Sul, “Multi-level operation of triple two-level PWM converters,” Proc. of IEEE Energy Conversion Congress and Exposition (ECCE’2015), 2015, pp. 4283-4289.

[20] V.F. Pires, A. Cordeiro, D. Foito, and J.F. Silva, “Three-phase multi-level inverter for grid-connected distributed photovoltaic systems based in three three-phase two-level inverters,” Solar Energy, vol. 174, 2018, pp. 1026-1034.

[21] V. Oleschuk and F. Barrero, “Standard and non-standard approaches for voltage synchronization of drive inverters with space-vector PWM: A survey,” International Review of Electrical Engineering, vol. 9, no. 4, 2014, pp. 688-707.

[22] V. Oleschuk and V. Ermuratskii, Dual Inverters with Synchronized Modulation for Transformer-Based Photovoltaic Installations, Chapter of the book “Renewable Energy. Selected Issues”, vol. 2, Cambridge Scholar Publishing, 2016, pp. 192-205.

[23] V. Oleschuk, V. Ermuratskii, and M. Pastor, “Alternative methods of synchronous space-vector PWM for transport-oriented converters and drives,” Proc. of IEEE Int’l Conf on Electrical Drives and Power Electronics (EDPE’2019), 2019, pp. 327-334.

[24] V. Oleschuk, V. Ermuratskii, and F. Barrero, “Multilevel installation based on voltage source inverters controlled by synchronous multi-zone PWM,” Proc. of IEEE Int’l Conf. on Electromechanical and Energy Systems (SIELMEN’2019), 2019, pp. 158-165.

[25] V. Oleschuk and V. Ermuratskii, “Synchronous balanced regulation of multiphase system on the base of modulated diode-clamped inverters,” Technical Electrodynamics, no. 5, 2019, pp. 27-35.

[26] V. Oleschuk and Ermuratskii, “Open-end winding multiphase installation regulated by modified techniques of space-vector PWM,” Proc. of IEEE Ukrainian Conf. on Electrical and Computing Engineering (UKRCON’2019), 2019, pp. 299-304.

[27] V. Oleschuk and V. Ermuratskii, ”Power balanced adjustment of quad-inverter installation with modified discontinuous PWM,” Problems of the Regional Energetics, № 1-3 (42), 2019, pp. 35-42.

[28] V. Oleschuk, V. Ermuratskii, and M. Pastor, “Synchronous adjustment of modular converter based on diode-clamped inverters with multi-zone PWM,” Proc. of IEEE Int’l Conf on Electrical Drives and Power Electronics (EDPE’2019), 2019, pp. 379-384.

[29] V. Oleschuk and V. Ermuratskii, “Novel methods, schemes and techniques of synchronous modulation for control of power conversion systems for transport: An Overview,” Proc. of IEEE Electrical Vehicle Conf. (EV’2019), 2019, 6 p.

[30] V. Oleschuk and V. Ermuratskii, “Review of methods and techniques of space-vector PWM for dual and triple inverters of PV systems,” Proc. of IEEE Int’l Conf. on Electromechanical and Energy Systems (SIELMEN’2019), 2019, pp. 205-212.

[31] V. Oleschuk, V. Ermuratskii, and F. Barrero, “Synchronous balanced control of dual split-phase drive topology with PWM diode-clamped inverters,” Proc. of IEEE Ukrainian Conf. on Electrical and Computing Engineering (UKRCON’2019), 2019, pp. 375-381.

[32] V. Oleschuk and V. Ermuratskii, “Two-inverter-based photovoltaic installation adjusted by the modified scheme of space-vector modulation,” Technical Electrodynamics, no. 5, 2020, pp. 26-30.

[33] V. Oleschuk and V. Ermuratskii, “PWM switching strategy of three-phase inverters for synchronous control of double-delta-winding system,” Proc. of IEEE Int’l Conf. KhPI Week on Advanced Technology 2020, 2020, pp. 268-272.

[34] V. Oleschuk and V. Ermuratskii, “Synchronous PWM regulation of inverters of drive installation with two stator windings of electrical motor,” Problems of the Regionl Energetics, №4 (48), 2020, pp. 1-10.

[35] V. Oleschuk and V. Ermuratskii, “Double-delta-winding system with neutral-point-clamped converters controlled by synchronous multi-zone PWM,” Proceedings of the Institute of Electrodynamics of the National Academy of Sciences of Ukraine, issue 56, 2020, pp. 59-63.

[36] V. Oleschuk, V. Ermuratskii, and I. Vasiliev, “Review of overmodulation control techniques of drive inverters with synchronous space-vector PWM,” Proc. of IEEE Int’l Conf. on Development and Application Systems (DAS’2020), 2020, pp. 98-105.

[37] V. Oleschuk and I. Vasiliev, “Motor drive system with double-delta-sourced stator winding and two modulated NPC converters,” Proc. of IEEE Int’l Conf. KhPI Week on Advanced Technology 2020, 2020, pp. 357-362.

[38] V. Oleschuk, M. Tirsu, V. Galbura, and I. Vasiliev, “Transformer-based PV system with modified techniques of PWM of diode-clamped inverters,” Proc. of IEEE Int’l Conf. on Development and Application Systems (DAS’2020), 2020, pp. 106-111.

[39] V. Oleschuk, I. Vasiliev, and G. Griva, “Overmodulation operation of two-level PWM inverters of photovoltaic system with double-delta configuration of power transformer,” Proc. of IEEE Int’l Conf. on Modern Power Systems (MPS’2021), 2021, 5 p.

[40] V. Oleschuk, “Strategies, schemes, and algorithms of synchronous space-vector PWM for voltage source inverters of open-end winding motor drives: An overview,” Proc. of IEEE Int’l Conf. on Electromechanical and Energy Systems (SIELMEN’2021), 2021, pp. 69-75.

[41] V. Oleschuk, I. Vasiliev, G. Griva, and F. Spertino, “Schemes and techniques of synchronous modulation of PV inverters with high modulation indices: A survey,” Proc. of IEEE Int’l Symp. on Advanced Topics of Electrical Engineering (ATEE’2021), 2021, 6 p.

[42] V. Oleschuk, “Methods and techniques of synchronous multi-zone modulation for the control of power electronic converters for electric transport and photovoltaic systems,” Akademos, № 4 (63), 2021, pp. 37-47.